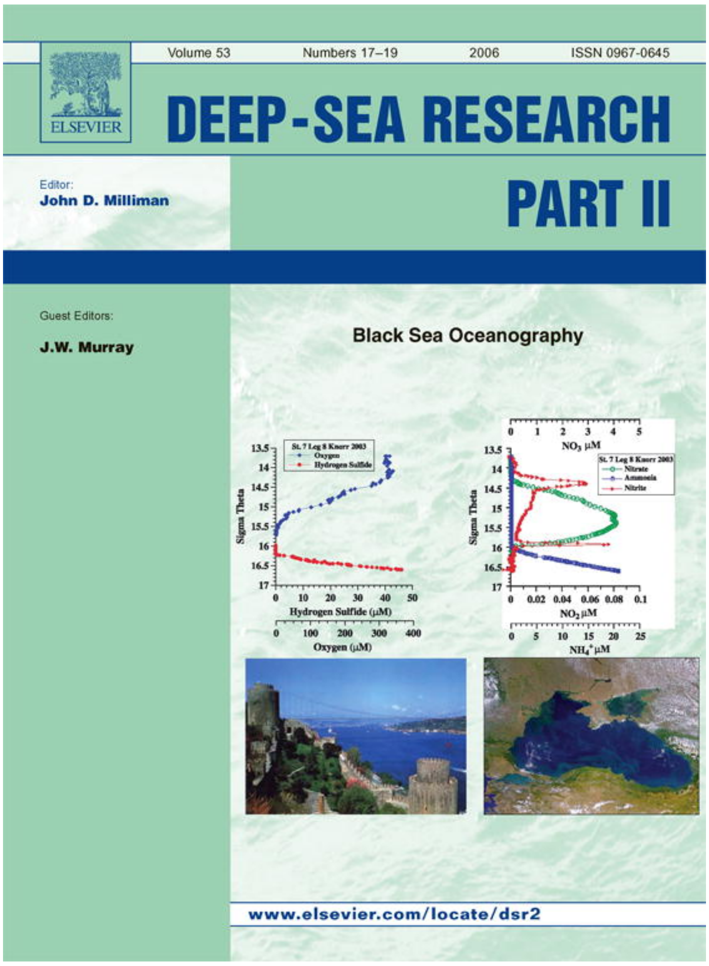
Volume 53
Numbers 17–19
2006
ISSN 0967-0645
ELSEVIER
DEEP-SEA RESEARCH
PART II
Editor:
John D. Milliman
Guest Editors:
J.W. Murray
Black Sea Oceanography
www.elsevier.com/locate/dsr2

Available online at www.sciencedirect.com
ScienceDirect
ELSEVIER
Deep-Sea Research II 53 (2006) 1923–1933
DEEP-SEA RESEARCH
PART II
www.elsevier.com/locate/dsr2

Comparision of in situ and satellite-derived chlorophyll pigment concentrations, and impact of phytoplankton bloom on the suboxic layer structure in the western Black Sea during May–June 2001

Temel Oguz*, Dilek Ediger

Institute of Marine Sciences, Middle East Technical University, Erdemli, Turkey

Received 1 September 2004; accepted 3 July 2006

Abstract

CTD and chlorophyll data collected during May–June 2001 R.V. *Knorr* and June 2001 R.V. *Bilim* cruises have been complemented by satellite altimeter sea-level anomaly, AVHRR sea-surface temperature and SeaWiFS chlorophyll data sets in order to infer temporal evolution and spatial variability of the circulation, water mass, and chlorophyll pigment concentration in the western Black Sea. Four specific features of the upper layer water-column physical and biogeochemical structures have been addressed in the present study. (i) A broader view of the large- and mesoscale-circulation characteristics, and thus more detailed interpretation of the limited set of measurements was provided by the use of satellite data; (ii) no appreciable Cold Intermediate Layer was detected in response to mild winter conditions prevailing over the basin prior to the cruise. The mild winter in 2001 was in fact prolongation of the similar winter conditions persistently observed during the second half of the 1990s; (iii) a weak phytoplankton bloom development was initiated along the peripheral zone towards the end of May, and then expanded over the entire western basin during the mid-June, soon after the completion of the R.V. *Knorr* surveys. The R.V. *Bilim* survey was able to partially capture this intense bloom phase. The SeaWiFS chlorophyll algorithm overestimated surface chlorophyll concentrations by a factor of 4 with respect to in situ measurements within four different regions of the western Black Sea (the southern coastal and Rim Current zones, the interior basin and the northwestern shelf); (iv) An immediate impact of the enhanced plankton activity was increased oxygen consumption within the upper 75 m of the water column due to remineralization of the increased flux of particulate organic material. This process apparently caused an upward rise of the upper boundary of the suboxic zone to shallower depths and lower density levels. It was located at sigma-t levels of $\sigma_t \sim 15.2$–$15.3\,\mathrm{kg\,m^{-3}}$ within the cyclonic western central basin, at $\sigma_t \sim 15.4\,\mathrm{kg\,m^{-3}}$ within the anticyclonic Sevastopol eddy and at $\sigma_t \sim 15.6\,\mathrm{kg\,m^{-3}}$ within the anticyclonic southern coastal zone. The previous assertion of the stability of the SOL upper boundary position at $\sigma_t \sim 15.6\,\mathrm{kg\,m^{-3}}$ irrespective of the seasons and circulation features (i.e. geographical locations) is therefore not supported by the May–June 2001 data set. It suggests that temporal and spatial variability in the SOL occurs during the year depending on varying local conditions imposed by the physical and biogeochemical processes.

Keywords: Black Sea; Chlorophyll pigment; SeaWiFS chlorophyll data; AVHRR sea surface temperature; Cold intermediate layer; Suboxic layer

*Corresponding author. Tel.: +90 324 521 2406; fax: +90 324 521 2327.
E-mail address: oguz@ims.metu.edu.tr (T. Oguz).

0967-0645/$ - see front matter © 2006 Elsevier Ltd. All rights reserved.
doi:10.1016/j.dsr2.2006.07.001

1. Introduction

The Black Sea ecosystem, altered drastically by impacts of climate change, eutrophication, overfishing and large population growth of gelatinous and opportunistic species, has been studied intensively by means of some international programs during the last two decades. The earliest example of international collaborative efforts was the first US-Turkish expedition of the R.V. *Knorr* during 1988 (Murray, 1991). The international collaborations made possible organization of some multi-ship field surveys, as well as interdisciplinary modelling and retrospective data analysis studies, throughout the 1990s (Ozsoy and Mikaelyan, 1997; Ivanov and Oguz, 1998; Besiktepe et al., 1999; Lancelot et al., 2002). As reviewed by Oguz et al. (2004), all these studies have brought a new perspective to our perception and understanding of the Black Sea circulation and biogeochemistry. The circulation system was found to involve a spatially complex structure dominated by mesoscale features instead of a simple twin-gyre, quasi-permanent circulation. The efficiency of such a mesoscale-dominated circulation system on material transport across the basin was observed to be significant (Oguz et al., 2002). The vertical biogeochemical pump included a succession of diatom, dinoflagellate, coccolithophore and small phytoplankton blooms throughout the year (Oguz and Merico, 2006), and accompanying highly efficient remineralization—ammonification—nitrificaton cycle within ~50–75 m depth range of the water column, followed further below by the reduced nitrate and oxygen depleted suboxic layer and oxidation–reduction reactions across the suboxic–anoxic interface (Oguz et al., 2000; Murray et al., 2005).

As a part of ongoing research initiatives in the Black Sea, a second US-Turkish cruise was conducted during 22 May–10 June 2001 in the western basin using R.V. *Knorr*. The major emphasis of the survey was to perform detailed biogeochemical measurements at dynamically different sites of the Black Sea, such as the Bosphorus exit region with maximum Mediterranean underflow influence, the northwestern shelf, the interior basin, the topographic slope zones on the southern side (e.g., Sakarya Canyon region), and the northern side (e.g., Danube Fan region) of the western interior. In the R.V. *Knorr* surveys, the station network (Fig. 1), however, was not sufficiently dense enough to deduce details of the horizontal circulation struc-

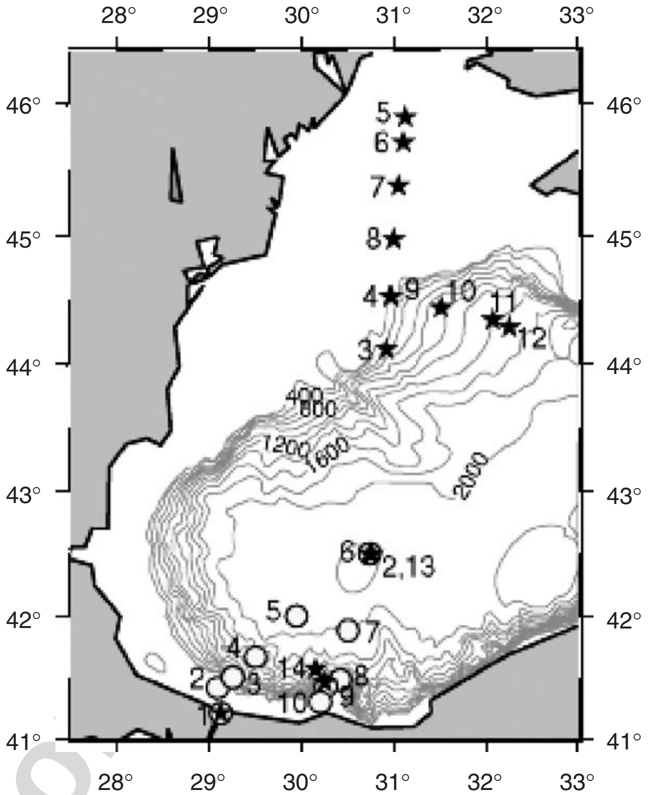

Fig. 1. Bathymetry and location map of stations covered in the first leg (circles) and the second leg (stars) of the R.V. *Knorr* 2001 survey in the western Black Sea. The bathymetry contours vary from 100 to 2000 m, and the contours from 200 to 2000 m are depicted at an interval of 200 m.

tures and thermohaline properties, as well as their impacts on biogeochemical characteristics. In the companion R.V. *Bilim* survey, the station network was more dense, but limited to the southwestern part of the western basin. In the present paper, utilizing satellite-derived altimeter sea-level anomaly, AVHRR sea-surface temperature, and SeaWiFS surface chlorophyll concentration data sets (Section 2), the flow and stratification characteristics of the western basin are documented and compared with in situ chlorophyll concentrations measured during the R.V. *Knorr* surveys. Impact of the phytoplankton bloom and the subsequent enhanced remineralization cycle on the SOL structure is presented.

2. Data collection and analysis

The station network of the R.V. *Knorr* 2001 Black Sea cruise (Fig. 1) was carried out in two legs. The first leg (23–31 May 2001) occupied stations in the western central basin, the Bosphorus exit region, and the shelf-slope zone to its east. Second leg (2–9

June 2001) included measurements within the northwestern shelf-slope zone as well as some repeated measurements at the western central station, and some coastal stations in the south. The R.V. *Bilim* 2001 cruise was conducted between 23 May and 18 June within the southwestern Black Sea. The CTD measurements were obtained using SeaBird SBE-9 sensors, and the entire data set in 1 m bin-averaged form is documented at the URL site http://oceanweb.ocean.washington.edu/cruises/Knorr2001/.

The daily sea-level anomaly (SLA) data relative to a 6-year (January 1993–January 1999) mean were given at http://las.aviso.oceanobs.com/las/servlets/datasets once a week centered at 23 May, 30 May and 6 June 2001 by the merged altimeter measurements of the Topex-Poseidon and ERS2 satellite passes over the region. The original data, provided on a Mercator 1/3° grid, are optimally interpolated to a 0.1° grid, and then superimposed onto the mean sea-level height obtained from the climatological hydrographic data (Korotaev et al., 2003). The horizontal current components are computed by assuming the geostrophic balance between the Coriolis and pressure gradient forces. The sea-surface temperature (SST) data are derived from weekly, 9-km gridded NOAA/NASA AVHRR Oceans Pathfinder data set retrieved at the URL site http://poet.jpl.nasa.gov. Similarly, the daily 9-km gridded chlorophyll concentration data set is obtained by the Distributed Active Archive Center at the Goddard Space Flight Center at http://eosdata.gsfc.nasa.gov/data/dataset/SEAWIFS/. The SeaWiFS algorithms are known to be more appropriate for the case 1 open ocean waters, and to contain serious errors for case 2 waters, such as the Black Sea, due to the problems of atmospheric correction and high turbidity. We consider that qualitative interpretations of images will not be altered by these possible error sources. Chlorophyll concentrations estimated by the SeaWiFS algorithm OC4 and obtained directly by in situ measurements are compared in Section 5 to assess the magnitude of error in the Black Sea SeaWiFS chlorophyll estimations.

Water samples for chlorophyll measurements were collected with 5-l Niskin bottles on a Rosette configured with a Sea-Bird CTD probe. Seawater samples (1–2 l) were filtered using GF/F glass-fibre filters, which were homogenized and extracted in 90% acetone solutions. The total chlorophyll contents of particle-free solutions were measured by the fluorometric method (UNESCO, 1994), using a Hitachi F-3000 Model fluorometer (analytical precision: 8% and detection limit: 0.01 $\mu g\, l^{-1}$) and a commercially available standard from Sigma. Water samples for measuring dissolved oxygen concentrations were collected by a pump cast sampler, and analysed by the traditional Winkler method. For further details on the data collection and processing methodology, we refer to the URL site www.ocean.washington.edu/cruises/Knorr 2001.

3. Flow and stratification characteristics

Flow fields (Fig. 2A–C) obtained from weekly composite altimeter data sets centered at 23 May, 30 May, and 6 June 2001 reflect typical characteristics of the Black Sea general circulation system (Korotaev et al., 2003), involving a cyclonic interior

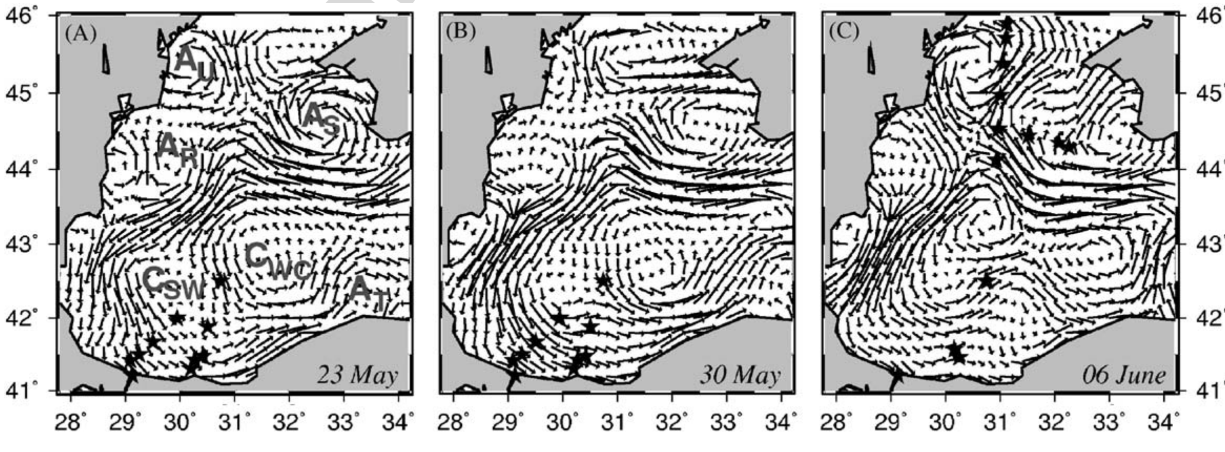

Fig. 2. Evolution of the flow field in the western basin estimated via the geostrophic balance by the merged weekly sea-level anomaly data from Topex-Poseidon and ERS-II altimeters centered during (A) 23 May, (B) 30 May, and (C) 6 June 2001. The station locations visited during the first leg of the R.V. *Knorr* cruise are shown in the first two plots and during the second leg in the last plot.

cell, the Rim Current circulating along the periphery, as well as a series of cyclonic and anticyclonic mesoscale eddies embeded within this system. The circulations for 23 May 2001 (Fig. 2A) and 30 May 2001 (Fig. 2B) resemble each other closely. The Rim Current splits into three branches to the southwest of the Crimean Peninsula. The main branch flowing first westward exhibits a large meander towards the northwestern shelf and then deflects south towards the Turkish coast. One of the remaining two branches proceeds northward and supports the Sevastopol anticyclonic eddy A_S. The other one deflects southward from the middle of the western basin and divides the interior cyclonic cell into two cyclones identified in Fig. 2A,B by C_{SW} and C_{WC}. The Rim Current along the Turkish coast also undergoes a large meander with an anticyclonic eddy A_T on its coastal side. In addition to the Sevastopol anticyclone, the northwestern shelf circulation is composed by three interconnected eddies; the cyclone C_N to the north of the Sevastopol eddy, and two anticyclones A_U and A_R along the western coast. This flow system is almost preserved during the subsequent week (Fig. 2B) except formation of a second meander along the Turkish coast along 31°E longitude and a slight eastward propogation of the whole system in the southern half and westward in the northern half of the basin.

In terms of the flow and stratification properties, stations 2, 3, and 4 occupying the shelf-slope zone outside the Bosphorus exit visited during the first 3 days of the first leg of R.V. *Knorr* cruise lie along the Rim Current zone with predominantly anticyclonic character, similar to the shelf-slope stations 8–10 covered during the latter part of first leg. The western central station 6 in the cyclonic interior basin lies along the southern branch of the Rim Current, and thus, as shown below, its cyclonic character is not as strong as the one visited during the R.V. *Knorr* 1988 survey (Murray et al., 1989). The same also applies for stations 5 and 7 situated along the offshore flank of the Rim Current flowing along the south coast.

The circulation for 6 June 2001 showed some changes and reorganization of the flow field (Fig. 2C). Within the northern half of the basin, the anticyclonic eddies A_R and A_S become larger and stronger and the cyclonic eddy A_N moves further westward and replaces the anticyclone A_U. Stations 3–9 occupied during the second leg along 31°E longitude in the northwestern shelf-slope region lie along the northward branch of the Rim Current, whereas stations 10–12 are located inside the Sevastopol anticyclone A_S. Two meanders of the southern coast amplify, penetrate more towards the interior, and establish contacts with the northern branch of the Rim Current. While the meander near the eastern end of the analysis region decouples the western interior from rest of the basin, the other meander located approximately between 31° and 32°E longitudes splits the western interior into two separate gyres. The western central station of the previous leg, which is visited twice during the early and late phases of second leg (stations 2 and 13 in Fig. 1), lies along the offshore periphery of the first Rim Current meander.

The AVHRR daily sea-surface temperature (SST) patterns also reveal some distinct features of the circulation system described above. But, the daily patterns are partially masked by cloud coverage and therefore are not particularly useful to infer a broad view of regional SST characteristics. Weekly composites overcome this deficiency at the expense of loosing some details of the flow structure. They are, however, adequate for our purpose of describing major regional changes in the daily SST distributions during the cruise period. The weekly composite SST patterns for the periods of 26 May–1 June 2001 and 2–9 June 2001, corresponding to first and second legs, respectively, are shown in Fig. 3A and B. The SST field given in Fig. 3A reveals temperature variations in the range 16.5–18.2 °C along the western and southern coasts. This region, characterized by the Rim Current zone (Fig. 2A and B), was separated from the relatively colder eastern and northern parts of the analysis region by

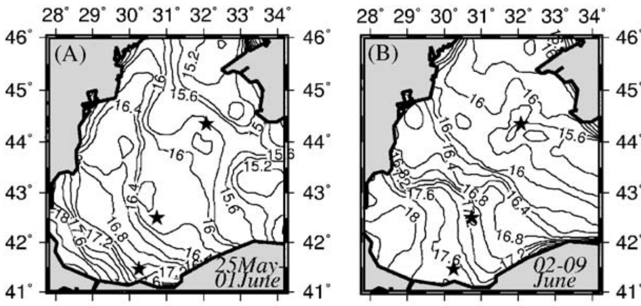

Fig. 3. Weekly composite SST distributions obtained from 9-km gridded NOAA/NASA AVHRR Oceans Pathfinder data set for (A) 26 May–2 June, (B) 3–10 June 2001 for the western Black Sea. The contours are drawn at an interval of 0.4 °C. The location of stations 11 (inside the Sevastopol eddy), 13 (within the western central gyre), 14 (near the south coast) are shown by stars.

a north-south oriented front, indicating that the region to the east of 31°E longitude had experienced some wind-induced cooling prior to the cruise. Temperature values less than 16.5 °C covered surface waters of the Sevastopol anticyclonic eddy and the cyclonic eddy situated its further north as well as the interior waters of the central basin near the eastern end of the analysis region (Fig. 3A). By entraining cold waters below the seasonal thermocline, the wind-induced mixing apparently resulted in a relatively uniform cold-water patch at the surface of these regions irrespective of the details of the flow field. Thus, surface waters of the anticyclonic eddies A_S, A_D and A_T are identified by relatively cold spots as if they represent cyclonic features. Their anticyclonic character, however, can be traced clearly below their surface mixed layers, as further documented below (see Fig. 4A).

A week later, during the second leg of the cruise, the SST structure (Fig. 3B) was transformed into two distinct spatially more uniform regions. The entire northeastern basin attained SST values of about 16 °C under the influence of strong west-northwesterly winds with a typical speed of about $10\,m\,s^{-1}$ that prevailed during 4–7 June 2001. On the contrary, the SSTs in the southern region were higher, about 17.0–18.0 °C. These two regions with two distinctly different SST characteristics were separated by a frontal zone extending along the northwest–southeast direction.The surface mixed layer of the eddies A_S, A_D and A_T continued to be capped by the relatively cold waters during this period.

Further details on the upper layer thermohaline structure are given by the temperature, salinity and density profiles (Fig. 4) at stations 13, 11, 14, representing the conditions within the western central, the Sevastopol eddy, and the southern coast, respectively. The profiles are chosen from the second leg, immediately after the wind mixing in the northern part of the basin. The measurements performed within the first leg and prior to the wind mixing event of the second leg also show similar vertical structures except some slight differences in the surface mixed layer properties. The largest differences in the temperature profiles were observed above the seasonal thermocline (Fig. 4A). The warmest temperatures in the mixed layer, greater than 17 °C, were observed at station 14 along the southern coast. The mixed layer deepened and cooled gradually towards the north as noted by temperatures of 15.5 and 14 °C within 20- and 30-m-thick mixed layers at station 13 (western central) and station 11 (Sevastopol anticyclone), respectively. The strongest contribution of the wind-induced mixing was also evident at the latter location by the presence of deeper and stronger seasonal thermocline with respect to other stations. Below 60 m depth, the role of surface cooling was no-longer effective and all three stations exhibit almost identical vertical structures for temperature.

The most important feature of the temperature profiles shown in Fig. 4A was the absense of a cold ıntermediate layer (CIL) characterized by temperatures lower than 8 °C below the seasonal thermocline. This was a common feature observed at all

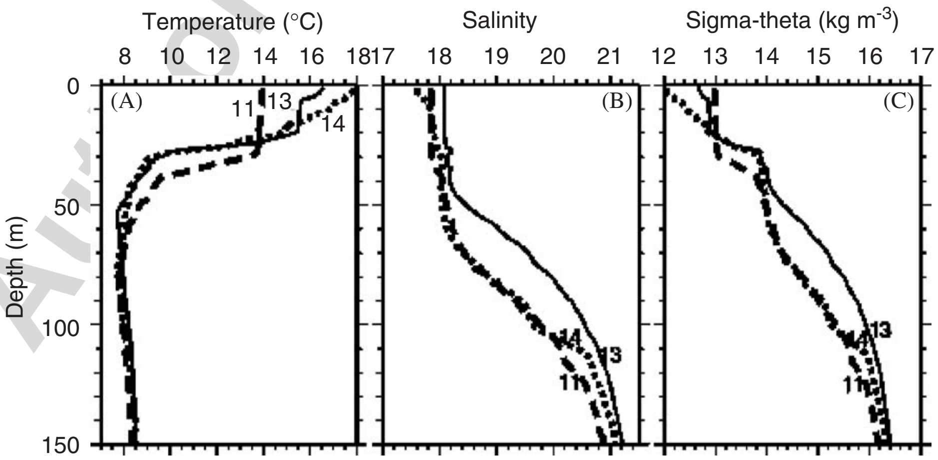

Fig. 4. Vertical profiles of (A) temperature (in °C), (B) salinity (unitless), (C) sigma-theta (in $kg\,m^{-3}$) measured within the uppermost 150-m layer of the water column measured in second leg at station 11 (Sevastopol anticyclone, 6 June, broken line), station 13 (western central, 8 June, straight line), and station 14 (southern coast, 9 June, dots).

stations, and the coldest CIL temperatures measured during the 2001 cruise were around 7.75 °C within a thin layer of about 5–10 m around 50 m depth in the western central station. Even if the CIL was convectively formed in winter months (see Fig. 4B for the 50-m-thick homogeneous salinity layer), temperature of the winter mixed layer was around 8 °C throughout the basin as shown by the February 2001 AVHRR SST distribution (see Fig. 4 in Oguz et al., 2003). The gradual depletion of the CIL during the entire second half of the 1990s has been previously noted (see Fig. 5 of Oguz et al., 2003 for a set of temperature profiles measured at western central station during the 1990s as well as Knorr 2001 cruise).

The vertical salinity profiles reveal more pronounced differences between these three stations (Fig. 4B). The salinity at stations 11 and 14, located within the Sevastopol anticyclone and the southern Rim Current zone, respectively, were about 0.3 lower than that of the western central station within the 50-m-thick surface homogeneous layer. The subsequent layer up to the depth of 150 m constitutes the halocline region, with strongest salinity variations of the order of 3.0. These variations are steeper and confined into a narrower layer within the cyclonic western central station with respect to other two sites with an anticyclonic character.

The density profiles (Fig. 4C) are predominantly governed by temperature variations within the upper 30-m layer, below which the salinity controls the density structure. Thus, the cyclonic western central station had denser waters relative to the anticyclones at the same depths. For example, the position of $\sigma_t \sim 16.2\,\mathrm{kg\,m^{-3}}$ level, representing the lower boundary of the Suboxic Layer, occured approximately at 135 m for the southern coastal station and 150 m for the anticyclonic Sevastopol eddy station. Similarly, the depth of $\sigma_t \sim 15.6\,\mathrm{kg\,m^{-3}}$, often considered to represent upper boundary of the Suboxic Layer, was located at ~100 m in these two anticyclonic stations. For the western central station, the corresponding SOL boundaries were located at relatively shallower depths of 85 and 120 m. These depths at the western central station were at least 20 m deeper than the corresponding values of 50–60 and 90–100 m at the same station during the R.V. *Knorr* 1988 cruise (Murray et al., 1989). While the latter values signify a typical case when the interior of the western basin was dominated by a well-defined cyclonic circulation, the corresponding values for the western

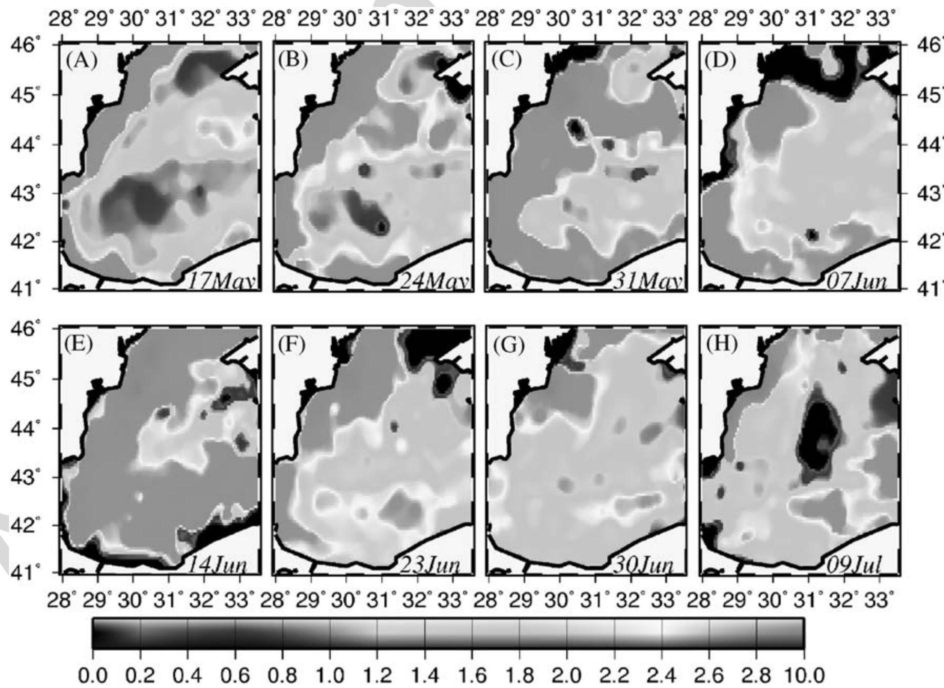

Fig. 5. Daily surface chlorophyll concentration (in mg m^{-3}) the western Black Sea obtained by the daily 9-km gridded data set of the distributed Active Archive Center at the Goddard Space Flight Center during (A) 17 May, (B) 24 May, (C) 31 May, (D) 7 June, (E) 14 June, (F) 23 June, (G) 30 June, (H) 9 July 2001. The contours are drawn at an interval of 0.2 up to 2.0 $\mathrm{mg\,m^{-3}}$. The regions in black color represent missing data points due to the cloud coverage.

central station of the R.V. *Knorr* 2001 survey represent weakly cyclonic or Rim Current transition zone flow condition. Station 7 of the first leg, also located in the deep part of the western basin to the south of western central station, possessed an anticyclonic character with the upper and lower SOL boundaries at 105 and 140 m, respectively (not shown).

4. Characteristics of surface chlorophyll pigment distribution, and comparison of measured and SeaWiFS derived chlorophyll concentrations

The SeaWiFS chlorophyll patterns shown in Fig. 5A–H describe different stages of the algae bloom activity during the 2 months period from mid-May to mid-July 2001. The first image for 17 May (Fig. 5A) indicates high chlorophyll concentrations ($>2.5\,\mathrm{mg\,m^{-3}}$) confined into the narrow belt along the western and southern coasts, as well as inside the Sevastopol eddy. The rest of the basin is characterized by chlorophyll concentrations less than $1.0\,\mathrm{mg\,m^{-3}}$, which in fact seems to represent the background state for this uncorrected SeaWiFS data set. Over the next 2 weeks, shown by 24 May and 31 May images in Figs. 5B and C, the production spread over most of the northwestern shelf along the south coast. The cyclonic part of the interior basin (Fig. 2B) continued to contain relatively lower chlorophyll concentrations of about $1.5\,\mathrm{mg\,m^{-3}}$. Some reduction in chlorophyll concentrations within the northern basin, including the region of the Sevastopol eddy, was noted in the subsequent week (Fig. 5D) due to vertical mixing and homegenisation of surface concentrations within the mixed layer immediately after passage of the storm. Once the storm-generated vertical mixing weakensed a few days later, the phytoplankton bloom flourished within the entire western basin during mid-June (Fig. 5E). The bloom terminated gradually within the second half of June from the interior towards the periphery (Figs. 5G–H). Thus, the SeaWiFS data suggest the peak state of the phytoplankton bloom occurred a week after completion of the second leg of R.V *Knorr* survey. The northwestern shelf stations, and stations inside the Sevastopol eddy and along the southern coast visited during second leg, however, should have captured the bloom signature reasonably well. The R.V. *Bilim* 2001 cruise, which took place within the southwestern Black Sea a week after the second leg of the R.V *Knorr* survey, also captured the bloom signature in the south (Table 1).

Basinwide coccolithophore blooms typically occurred in the Black Sea in the May–June periods of 1997–2002 (Cokacar et al., 2001, 2004). These are identified in Fig. 6 by pronounced peaks of monthly areal coccolith coverage as a percentage of the basin. Domination of coccolithophores with respect to other algae groups was further supported by an opposite variation of the basin-averaged SeaWiFS-derived chlorophyll concentrations during the same period (Fig. 6). The only case of the non-coccolithophore bloom event over the 1997–2002 period occurred in May–June 2001, was identified by a stronger chlorophyll pigment and weaker coccolith signature in Fig. 6. In fact, the pigment measurements as well as the microscopic analysis of water samples (Ediger et al., 2006) confirmed that the phytoplankton community structure in the western Black Sea was dominated of dinoflagellates in the May–June 2001.

Surface chlorophyll concentrations measured during R.V. *Knorr* 2001 and the R.V. *Bilim* 2001 surveys with the corresponding values provided by the SeaWiFS satellite sensor are compared in Table 1. Because of the presence of a phytoplankton bloom, these measurements are particularly useful for assessment and calibration of the SeaWiFS-derived chlorophyll estimates. The data given in Table 1 have been arranged in four groups, representing the measurements along the southern coast, within the adjacent Rim Current zone, the northwestern shelf, and central waters of the western basin. The measurements within the southern Black Sea revealed in situ concentrations as high as $0.94\,\mathrm{mg\,m^{-3}}$, but generally varied around the mean value of $0.56\pm0.19\,\mathrm{mg\,m^{-3}}$. The corresponding SeaWiFS estimates have the mean value of $2.4\pm0.16\,\mathrm{mg\,m^{-3}}$, which is roughly 4.3 times higher than the in situ measurements. The mean values of the in situ and SeaWiFS chlorophyll concentrations for the adjacent southern Rim Current zone are, respectively, 0.50 ± 0.12 and $2.3\pm0.19\,\mathrm{mg\,m^{-3}}$ resulting in the ratio of 4.5. The ratio is 4.2 for the interior basin, and 3.8 for the northwestern shelf-slope region. Thus, these measurements suggest an overestimation of the SeaWiFS-derived chlorophyll concentration consistently by a factor of 4 at all regions of the western basin. More realistic chlorophyll distributions would thus be given in Fig. 5A–H if the SeaWiFS derived chlorophyll estimates were divided by 4.

Table 1
Comparison in situ and SeaWiFS-estimated chlorophyll concentrations at selected stations during the R.V Knorr and R.V Bilim May–June 2001 cruises

Latitude	Longitude	Region	Date	Cruise	Chl (in situ)	Chl (SeaWiFS)	Ratio
41°28′	30°16′	S-Coast	30-May	Knorr-1	0.30	2.6	
41°27′	30°15′	S-Coast	09-Jun	Knorr-2	0.33	2.55	
41°15′	29°45′	S-Coast	16-Jun	Bilim-2	0.54	2.6	
41°15′	30°15′	S-Coast	16-Jun	Bilim-2	0.45	2.1	
41°15′	30°45′	S-Coast	16-Jun	Bilim-2	0.70	2.3	
41°30′	30°45′	S-Coast	17-Jun	Bilim-2	0.94	2.4	
41°30′	31°15′	S-Coast	17-Jun	Bilim-2	0.58	2.3	
41°27′	31°30′	S-Coast	17-Jun	Bilim-2	0.62	2.5	
41°30′	31°45′	S-Coast	17-Jun	Bilim-2	0.62	2.4	
					0.56±0.19	2.4±0.16	4.28
41°50′	29°15′	S-Rim	23-May	Bilim-1	0.42	1.9	
41°50′	31°45′	S-Rim	26-May	Bilim-1	0.40	2.3	
41°50′	31°45′	S-Rim	17-Jun	Bilim-2	0.36	2.4	
41°40′	31°30′	S-Rim	17-Jun	Bilim-2	0.68	2.2	
41°50′	30°15′	S-Rim	18-Jun	Bilim-2	0.61	2.3	
41°50′	29°45′	S-Rim	18-Jun	Bilim-2	0.48	2.4	
41°44′	29°40′	S-Rim	18-Jun	Bilim-2	0.62	2.5	
					0.50±0.12	2.3±0.19	4.5
42°30′	30°50′	Interior	26-May	Knorr-1	0.14	1.2	
42°30′	30°46′	Interior	01-Jun	Knorr-2	0.32	1.3	
42°30′	30°46′	Interior	03-Jun	Knorr-2	0.15	1.1	
42°30′	31°45′	Interior	25-May	Bilim-1	0.54	1.3	
					0.29±0.18	1.22±0.09	4.2
44°08′	30°55′	Shelf	04-Jun	Knorr-2	0.26	2.9	
44°26′	31°30′	Shelf	06-Jun	Knorr-2	0.48	1.9	
44°21′	32°04′	Shelf	06-Jun	Knorr-2	0.55	1.6	
44°21′	32°04′	Shelf	06-Jun	Knorr-2	0.41	1.7	
45°23′	31°03′	Shelf	05-Jun	Knorr-2	0.69	1.8	
44°58′	31°00′	Shelf	05-Jun	Knorr-2	0.29	2.4	
44°32′	30°58′	Shelf	06-Jun	Knorr-2	0.64	2.6	
45°54′	30°57′	Shelf	04-Jun	Knorr-2	1.83	4.5	
					0.64±0.5	2.42±0.95	3.78

The coordinates and the specific regions of stations, the date of measurements as well as the ratio of SeaWiFS and in situ chlorophyll concentrations for each region are also indicated.

Large differences between in situ chlorophyll measurements and their satellite-derived estimates by means of various ocean-color sensors for case 2 waters in general, and the Black Sea in particular already have been noted by Bricaud et al. (2002), Kopelevich et al. (2002), Gregg and Casey (2004), and Sancak et al. (2005). Poor agreement is generally attributed to the drawback of chlorophyll algorithms due to richness of chromophoric dissolved organic matter, phytoplankton species diversity and absorbing aerosols in such case 2 waters. Most previous studies lacked sufficiently dense measurements acquired during pytoplankton bloom events in the Black Sea. The present study was able to cover a wide range of chlorophyll concentrations and therefore determined a specific error estimate for the satellite-derived surface chlorophyll data.

5. Impact of phytoplankton bloom on the SOL structure

The previous observations (Murray et al., 1989, 1995; Tugrul et al., 1992; Saydam et al., 1993; Konovalov and Murray, 2001) reported confinement of the suboxic layer (SOL) between two isopycnic levels of $\sigma_t \sim 15.6$ and $16.2\,kg\,m^{-3}$, irrespective of the season and geographical region of the sea. Reanalyzing the existing data and complementing them by model simulations, Oguz (2002) showed that that while the lower boundary of the SOL remains isopycnally uniform for all regions of the sea, the position of its upper boundary (characterized customarily by 10 μM oxygen concentration) may vary from $\sigma_t \sim 15.6\,\mathrm{kg\,m^{-3}}$ in cyclones to $\sigma_t \sim 15.9\,\mathrm{kg\,m^{-3}}$ in anticyclones. The deeper position of the SOL upper boundary within the anticyclones was suggested to be related to their stronger net downward flux of oxygen (i.e. the sum of diffusive and advective contributions).

In addition to the contribution by physical processes, the SOL structure also is expected to vary temporally by the impact of biological processes. One impact of the enhanced phytoplankton activity in the water column, is that the Knorr 2001 data set has consistently shown high oxygen consumption and thus a shoaling of the upper boundary of the SOL. For example, Fig. 7A shows oxygen measurements within the western central station at three different times: during 28 May (station 6, leg 1), 2 June (station 2, the begining of leg 2), 8 June (station 13, the end of leg 2). As already shown in Fig. 5, the time of these measurements represented a gradually intensifying phytoplankton bloom event within the central basin. As the bloom progressed, a greater rate of particulate matter remineralization in the chemocline zone apparently leads to an increased rate of oxygen consumption. This process is clearly noted in Fig. 7A by gradual change in the position of the oxycline and the upper boundary of the SOL from $\sigma_t \sim 15.3\,\mathrm{kg\,m^{-3}}$ to $\sigma_t \sim 15.15\,\mathrm{kg\,m^{-3}}$. Considering the fact that the mature phase of the bloom occured a week later than the measurements (8 June 2001) at station 13, the upper boundary of the SOL would be expected to shoal toward shallower depths and density levels during the subsequent few weeks. On the other hand, the upper boundary of the SOL occurred approximately at $\sigma_t \sim 15.4\,\mathrm{kg\,m^{-3}}$ level in the Sevastopol anticyclonic eddy (stations 11 and 12, 6–7 June 2001) (Fig. 7B), and at $\sigma_t \sim 15.5\,\mathrm{kg\,m^{-3}}$ level at the southern coastal station 9 of leg 1 (29 May 2001) and station 14 of leg 2 (9 June 2001) (Fig. 7C). The upper SOL boundary shifted upward by about $\sigma_t \sim 0.3$–$0.4\,\mathrm{kg\,m^{-3}}$ both in the cyclonic and anticyclonic regions as compared with its position reported previously by earlier measurements (Murray et al., 1989; Tugrul et al., 1992;

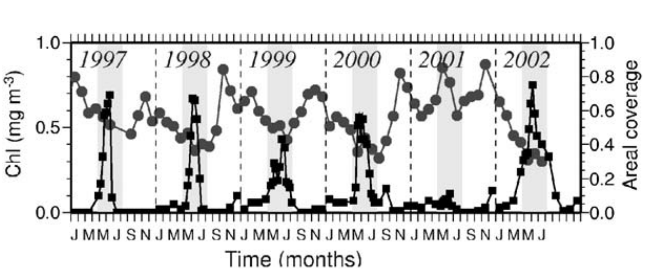

Fig. 6. Time series of the monthly, basin-average surface chlorophyll ($\mathrm{mg\,m^{-3}}$) distribution obtained by 9-km gridded SeaWiFS and OCTS data (dots), and the areal coccolith coverage as a percentage of the basin (squares) for the 1997–2002 period in the Black Sea (after Cokacar et al., 2004). The gray-shaded zones represent the May–July period in which coccolithophore blooms normally occur. The basin-averaging in the chlorophyll and coccolith concentrations exclude the coastal regions shallower than 200 m. The OCTS data covers only the January–May period of 1997.

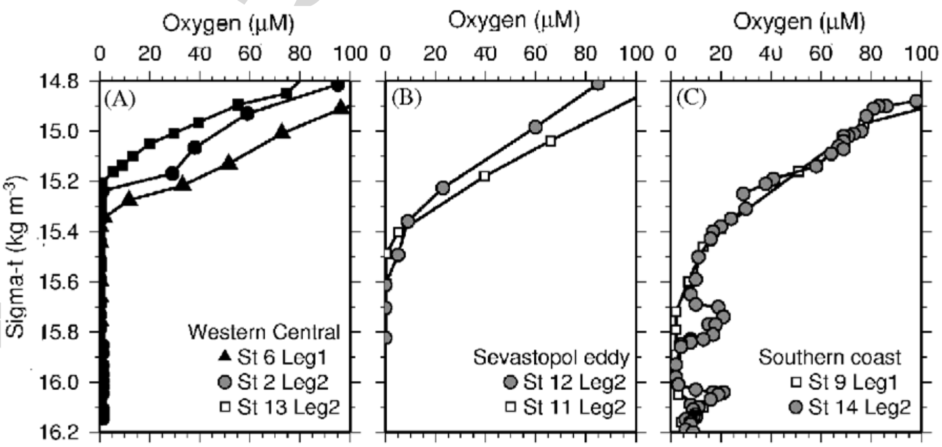

Fig. 7. Dissolved oxygen (in μM) profiles against sigma-t ($\mathrm{kg\,m^{-3}}$) measured during the R.V. *Knorr* May–June 2001 cruise (A) within the western central, at station 6—leg 1 during 27 May 2001 (triangles); station 2—leg 2 during 2 June (dots); station 13 during 8 June (squares), (B) within the Sevastopol eddy, at station 11—leg 2 during 6 June (squares); station 12—leg 2 during 7 June (dots), (C) near the southern coast, at station 9—leg 1 during 29 May (squares); station 14—leg 2 during 9 June (dots). The oxygen measurements at station 9 in the third plot also show relativel oxygen rich intermittent lateral intrusions of the Mediterranean underflow.

Saydam et al., 1993; Basturk et al., 1997). The difference of $\Delta\sigma_t \sim 0.3$–$0.4\,kg\,m^{-3}$ suggested earlier by Oguz (2002) between the positions of the upper SOL boundary in the cyclonic and anticyclonic regions was confirmed during these measurements.

The oxygen profiles in Fig. 7C show lenses of oxygen concentrations greater than 10 μM within the SOL and its interface with the anoxic layer. These relatively high concentrations are evidence of intrusions of relatively oxygen rich Mediterranean underflow entered into the Black Sea from the Bosphorus and spreaded within the southwestern Black Sea shelf-slope region at intermediate depths. More details on the lateral intrusion characteristics have been recently provided by Konovalov et al. (2003).

6. Summary and conclusions

The present study makes use of satellite-derived altimeter sea-level anomaly, AVHRR sea-surface temperature, and the SeaWiFS chlorophyll data to complement some findings of the R.V. *Knorr* and R.V. *Bilim* surveys conducted during May–June 2001 in the western Black Sea basin. Our analysis suggests the following features of the Black Sea flow and biogeochemical structures:

(1) The upper layer circulation system involved a complex flow structure that evolved during the course of the survey period in terms sizes and locations of eddies and meanders of the Rim Current.
(2) Surface waters in the northern part of the basin were subjected to short-term wind-induced mixing, and subsequent surface cooling. As a result, the Sevastopol anticyclonic eddy cannot be identified by the AVHRR sea-surface temperature field alone, unless the altimeter data is used to see the water-column flow structure.
(3) The temperature vertical structure did not show any sign of recent CIL formation due to an apparently mild winter season prior to the survey. The coldest subsurface temperature was around 7.75 °C measured at the western central station. This observation was consistent with the steady warming in the Black Sea upper layer waters during winter months since 1995 at a rate of ~0.2 °C per year and the subsequent gradual erosion of the CIL structure (Oguz et al., 2003).
(4) The survey period was characterized by a phytoplankton bloom in the surface mixed layer. The bloom was initiated around the periphery of the western basin during the first leg, it spread towards the interior during the first week of June (i.e. during second leg of the R.V. *Knorr* cruise) and covered the entire western basin a week later (i.e. immediately after completion of the cruise).
(5) Chlorophyll concentrations obtained by the SeaWiFS algorithm overestimate with respect to the in situ measurements by a factor of ~4. This estimate is based on a wide coverage of chlorophyll concentrations. Even though earlier studies pointed out large differences between the measured and satellite estimated surface chlorophyll concentrations, this is the first opportunity to make a specific error estimate.
(6) The impacts of enhanced plankton activity on the biogeochemical pump are increased particulate organic matter content and export flux, more uniform nutrient concentrations within the water column (Coban-Yildiz, 2003; Coban-Yıldız et al., 2006), and upward rise of the SOL upper boundary by about $\Delta\sigma_t \sim 0.3$–$0.4\,kg\,m^{-3}$ both in the cyclonic and anticyclonic regions due to intense oxygen consumption during high rate of particle remineralization. A difference of $\Delta\sigma_t \sim 0.3$–$0.4\,kg\,m^{-3}$ in the upper SOL position between the cyclonic and anticyclonic regions, observed in earlier data sets, also was noted in the present data. So far, this unique data set suggest the presence of both temporal (e.g. monthly-to-seasonal) and regional variabilities of the upper SOL boundary, contrary to the existing view of its rather steady character throughout the year and the basin.

Acknowledgements

The altimeter data were produced by the CLS Space Ocean Division as part of the Environment and Climate EU ENACT project (EVK2-ct2001-00117) and with support from CNES. The SeaWiFS chlorophyll data are provided by the Distributed Active Archive Center at the Goddard Space Flight Center. We thank T. Cokacar for processing of the daily SeaWiFS chlorophyll data, and D. Yilmaz for in situ chlorophyll measurements.

References

Basturk, O., Tugrul, S., Konovalov, S.K., Salihoglu, I., 1997. Variations in the vertical structure of water chemistry within the three hydrodynamically different regions of the Black Sea.

In: Ozsoy, E., Mikaelyan, A.S. (Eds.), Sensitivity to Change: Black Sea, Baltic Sea and North Sea. NATO Sci. Partnership Sub-series 2. Vol. 27. Kluwer Academic Publishers, Dordrecht, pp. 183–196.

Besiktepe, S., Unluata, U., Bologa, A.S., 1999. Environmental degradation of the Black Sea: Challenges and Remedies. NATO ASI Series 2, Environmental Security-56. Kluwer Academic Publishers, Dordrecht, 393pp.

Bricaud, A., Bosc, E., Antoine, D., 2002. Algal biomass and sea surface temperature in the Mediterranean basin. Intercomparison of data from various satellite sensors, and implications for primary production estimates. Remote Sensing of Environment 81, 163–178.

Coban-Yildiz, Y., 2003. Nitrogen cycling in the Black Sea. PhD thesis, METU, Institute of Marine Sciences, Erdemli, Mersin, Turkey, 176pp.

Coban-Yıldız, Y., Fabbri, D., Baravelli, D., Vassura, I., Yilmaz, A., Tugrul, S., Eker-Develi, E., 2006. Analytical Pyrolysis of Suspended Particulate Organic Matter from the Black Sea Water Column.

Cokacar, T., Kubilay, N., Oguz, T., 2001. Structure of *Emiliania huxleyi* blooms in the Black Sea surface waters as detected by SeaWIFS imagery. Geophysical Research Letters 28 (24), 4607–4610.

Cokacar, T., Oguz, T., Kubilay, N., 2004. Interannual variability of the early summer coccolithophore blooms in the Black Sea: impacts of anthropogenic and climatic factors. Deep-Sea Research I 51, 1017–1031.

Ediger, D., Soydemir, N., Kıdeys, A., 2006. Estimation of phytoplankton biomass using HPLC pigment analysis in the southwestern Black Sea.

Gregg, W.W., Casey, N.W., 2004. Global and regional evaluation of the SeaWiFS chlorophyll data set. Remote Sensing of Environment 93, 463–479.

Ivanov, L., Oguz, T., 1998. Ecosystem Modeling as a Management Tool for the Black Sea. NATO ASI Series 2, Environmental Security-47. Kluwer Academic Publishers, Dordrecht, vol. 1, 377pp and vol. 2, 385pp.

Konovalov, S.K., Murray, J.W., 2001. Variations in the chemistry of the Black Sea on a time scale of decades (1960–1995). Journal of of Marine Systems 31, 217–243.

Konovalov, S.K., Luther III, G.W., Friederich, G.E., Nuzzio, D.B., Tebo, B.M., Murray, J.W., Oguz, T., Glazer, B., Trouwborst, R.E., Clement, B., Murray, K.W., Romanova, A., 2003. Lateral injection of oxygen with the Bosphorus plume-Fingers of oxidizing potential in the Black Sea. Limnology Oceanography 48 (6), 2369–2376.

Kopelevich, O.V., Sheberstov, S.V., Yunev, O., Basturk, O., Finenko, Z.Z., Nikinov, S., Vedernikov, V.I., 2002. Surface chlorophyll in the Black Sea over 1978–1986 derived from satellite and in situ data. Journal of Marine Systems 36, 145–160.

Korotaev, G.K., Oguz, T., Nikiforov, A., Koblinsky, J.C., 2003. Seasonal, interannual and mesoscale variability of the Black Sea upper layer circulation derived from altimeter data. Journal of Geophysical Research 108 (C4), 3122.

Lancelot, C., Martin, J.M., Panin, N., Zaitsev, Y., 2002. The North-western Black Sea: a pilot site to understand the complex interaction between human activities and the coastal environment. Estuarine, Coastal and Shelf Science 54, 279–283.

Murray, J.W., 1991. Black Sea Oceanography: Results from the 1988 Black Sea Expedition. Deep-Sea Research 38 (Suppl. 2A), 1266.

Murray, J.W., Jannash, H.W., Honjo, S., Anderson, R.F., Reeburgh, W.S., Top, Z., Friederich, G.E., Codispoti, L.A., Izdar, E., 1989. Unexpected changes in the oxic/anoxic interface in the Black Sea. Nature 338, 411–413.

Murray, J.W., Codispoti, L.A., Friederich, G.E., 1995. Redox Environments: The suboxic zone in the Black Sea. In: Huang, C.P., O'Melia, C., Morgan, J.J. (Eds.), Aquatic Chemistry. American Chemical Society, pp. 157–176.

Murray, J.W., Fuchsman, C., Kirkpatric, J., Paul, B., Konovalov, S.K., 2005. Species and δ^{15}N signatures of nitrogen transformations in the suboxic zone of the Black Sea. Oceanogrraphy 18, 36–47.

Oguz, T., 2002. Role of physical processes controlling oxycline and suboxic layer structure in the Black Sea, Global Biogeochem. Cycles 16, doi:10.1029/2001GB001465.

Oguz, T., Merico, A., 2006. Factors controlling the summer Emiliania huxleyi bloom in the Black Sea: a modeling study. Journal of Marine Systems 59, 173–188.

Oguz, T., Ducklow, H.W., Malanotte-Rizzoli, P., 2000. Modeling distinct vertical biogeochemical structure of the Black Sea: dynamical coupling of the oxic, suboxic and anoxic layers. Global Biogeochemical Cycles 14 (4), 1331–1352.

Oguz, T., Deshpande, A.G., Malanotte-Rizzoli, P., 2002. On the role of mesoscale processes controlling biological variability in the Black Sea: Inferrences from SEAWIFS-derived surface chlorophyll field. Continental Shelf Research 22, 1477–1492.

Oguz, T., Cokacar, T., Malanotte-Rizzoli, P., Ducklow, H.W., 2003. Climatic warming and accompanying changes in the ecological regime of the Black Sea during 1990s. Global Biogeochemical Cycles 17 (3), 1088.

Oguz, T., Tugrul, S., Kideys, A.E., Ediger, V., Kubilay, N., 2004. Physical and biogeochemical characteristics of the Black Sea. In: Robinson, A.R., Brink, K. (Eds.), The Sea. Vol. 14. pp. 1331–1369 (Chapter 33).

Ozsoy, E., Mikaelyan, A.S., 1997. Sensitivity to Change: Black Sea, Baltic Sea and North Sea, NATO Science. Partnership Sub-series 2, Vol. 27. Kluwer Academic Publishers, Dordrecht, 516pp.

Sancak, S., Besiktepe, S.T., Yılmaz, A., Lee, M., Frouin, R., 2005. Evaluation of SeaWiFS chlorophyll-a in the Black and Mediterranean Seas. International Journal of Remote Sensing 26, p. 2045–2060.

Saydam, C., Tugrul, S., Basturk, O., Oguz, T., 1993. Identification of the oxic/anoxic interface by isopycnal surfaces in the Black Sea. Deep-Sea Research 40, 1405–1412.

Tugrul, S., Basturk, O., Saydam, C., Yilmaz, A., 1992. The use of water density values as a label of chemical depth in the Black Sea. Nature 359, 137–139.

UNESCO, 1994. Protocols for the Joint Global Ocean Flux Study (JGOFS) Core Measurements, Intergovernmental Oceanographic Commission, Manual and Guides, 29 (Chapter 14).